

Resistance Switching Behavior of ZnO Resistive RAM (RRAM) with a Reduced Graphene Oxide capping layer

Cheng-Li Lin^a, Wei-Yi Chang^b, Yen-Lun Huang, Tse-Wen Wang, and Ke-Yu Hung

Department of Electronic Engineering, Feng Chia University, No. 100, Wenhwa Rd., Seatwen, Taichung, Taiwan 407, R.O.C.

Phone: +886-4-24517250 Ext. 4969 Fax: +886-4-24510405 ^aE-mail: clilin@fcu.edu.tw, ^bE-mail: weiyioh@hotmail.com

1. Instruction

Resistive RAM (RRAM) is one of the most promising technology for next generation nonvolatile memory technology due to the simple structure, high density and low power consumption [1,2]. Metal oxide based RRAM reveals superior high/low resistance switching behavior, such as HfO₂ and ZnO [3,4]. ZnO material can be as the application of the flexible and transparent electronic device [5,6]. In order to improve the switching performance. Some metal insertion or stack layer is also studied [6]. Recently, graphene and graphene oxide have attracted much attention as future conductor and RRAM, respectively, for flexible electric device [7]. Additionally, graphene is also can be as the reservoir to absorb and desorb the charged particle (oxygen ion) in the RRAM switching and improving the performance [8]. Little study investigates the effect of ZnO with graphene insertion electrode as the reservoir to improve the performance of ZnO RRAM for future transparent RRAM application.

In this work, we investigate the ZnO RRAM w/ and w/o graphene insertion between ZnO and metal electrode. The graphene film is fabricated in low temperature process by a spraying process using the reduced graphene oxide solution. In order to clarify the switching mechanism of the RRAM with graphene insertion, we also investigate the effect of bias-polarity in the RRAM switching.

2. Experimental

ZnO film (60 nm) was deposited on the Al/SiO₂/Si substrate using a sputtering system with a ZnO (99.99%) target. Following a multilayer reduced graphene oxide (rGO) film (15nm) deposited on the substrate by a spraying-on method via an rGO liquid solution. The spraying rate is 0.1 ml/min and round scanned 1 time at a substrate temperature of 100°C. Then, a top Al electrode with a diameter of 200μm was deposited by an E-beam system using a shadow-metal mask to pattern the top circular electrode. The schematic of the Al/rGO/ZnO/Al RRAM with rGO film capping layer is shown in Fig. 1. In addition, the w/o rGO film samples were also preparation. The electrical characteristics of the RRAMs were measured by an Agilent 4155C in bipolar operation mode. Firstly, negative and positive bias was applied to SET and RESET the RRAM, respectively. The third experiment is changed the bias polarity of SET/RESET to investigate the bias polarity effect on the RRAM with rGO film, this sample denoted (similar) as Al/ZnO/rGO/Al RRAM. The chemical composition and binding energy of rGO was identified by X-ray photoelectron spectroscopy (XPS) analysis.

3. Results and Discussion

Fig. 2 shows binding energy of the as-deposited rGO film, the C-C, C=O and C-O bonds appear in the figure, indicating the film reveals rGO film property with sp² orbit with less oxygen composition [7]. Fig. 3 shows IV curves of ZnO, rGO/ZnO, ZnO/rGO RRAMs in the first 10 times and 100th ~110th switching curves at a current compliance of 10 mA in the SET/RESET process. With rGO film devices show obvious current jumping behavior in SET process. Additionally, the Al/ZnO/rGO/Al RRAM reveals most stable switching curve [Fig. 3(e) and (f)]. Fig. 4 shows the endurance of various RRAMs at a read voltage of 0.1V. The rGO/ZnO RRAM shows larger resistance ratio ($R_{HRS/LRS}$), but the uniformity of HRS is worse and similar to w/o rGO RRAM. The ZnO/rGO RRAM shows the most stable HRS and stable ($R_{HRS/LRS}$) (Fig. 4c). Fig. 5 shows the box plots of HRS/LRS resistance for various RRAMs. Low resistance states are not affected by the rGO film insertion or not for three kinds of RRAM. It can be seen the ZnO RRAM w/o rGO film shows larger variation in the HRS and the $R_{HRS/LRS}$ is about 2.5 order calculated from the median value. For the rGO/ZnO RRAM shows higher $R_{HRS/LRS}$ (~ 5 order) (Fig. 5b). Additionally, the ZnO/rGO RRAM shows less variation in HRS and higher $R_{HRS/LRS}$ (~ 5 order) (Fig. 5c). From the above experimental results, the Al/ZnO/rGO/Al RRAM reveals the best performance. Additionally, the bias polarity

and the rGO film position (in the top or bottom) affects the switching behavior. Fig. 6 shows the SET/RESET voltages in the endurance. Obviously reduced variation of SET voltage is observed for the RRAM with rGO film [Fig 6(b) and (c)]. The box plot of SET/RESET voltages for various RRAMs is shown in Fig. 7. The SET voltage (amplitude) of the rGO/ZnO RRAM is slightly larger than that of ZnO/rGO RRAM. Additionally, the SET voltage is most stable for the ZnO/rGO RRAM (Fig.7c). Fig. 8 shows the retention of ZnO, rGO/ZnO, and ZnO/rGO RRAMs. The retention of the three kinds of RRAMs can pass ten years lifetime prediction without obvious HRS/LRS degradation. In order to study the current transport mechanism of HRS and LRS for the ZnO RRAM with rGO film, we re-plot the IV curve in the double logarithm scale and shown in Fig. 9. In LRSs of the three kinds of RRAMs, the slopes are near 1 and they belong to the Ohmic conduction mechanism [4]. For the ZnO RRAM w/o rGO film [Fig. 9(a)], the HRS slope is 1.10 and 1.83 at low and high bias voltage, respectively. This indicates the current transport mechanism is the space charge limit current (SCLC) [4,10]. Similar current conduction mechanism of SCLC at low and medium bias voltages for rGO/ZnO RRAM (Fig.9b). Larger slope (4.12) is at the high bias voltage, indicating the deeper traps appeared in the rGO/ZnO film [4]. Presumably, the rGO film possesses higher out-of-plane resistance [10], and the less oxygen functional group [11] led to the result. For the conduction mechanism of the ZnO/rGO RRAM, the slopes at low and high bias voltages are similar to the ZnO RRAM (1.09 and 1.85 vs. 1.10 and 1.83), presumably the current conduction is not affected by the rGO insertion.

According to the current conduction analysis, we propose a resistance switching model shown in Fig. 10 for ZnO RRAM with rGO film insertion and the bias polarity effect. For the ZnO RRAM w/o rGO film, the oxygen ions (negative ions) moved to bottom electrode at SET bias (negative bias) and left oxygen vacancies to form the conductive filament path (ON state). When RESET bias applied (positive) oxygen ions return back to the vacancies and to disconnect the conductive path (OFF state). Presumably, the bottom interface layer (ZnO/Al) is the key role for the oxygen absorption and desorption. For the rGO/ZnO RRAM, when SET bias applied on the top metal, the key role for the oxygen absorption and desorption is at the bottom, and the rGO affects the total resistance and decrease leakage current, not as the reservoir layer. When changing the SET bias as positive (equivalent to Al/ZnO/rGO/Al RRAM using the same negative SET bias in the top metal), the rGO film acts as the key reservoir layer and enhanced the RRAM performance.

4. Conclusion

This work investigates the ZnO RRAM w/ and w/o rGO film and the SET/RESET bias polarity effect. The rGO film insertion increases the HRS and the endurance up to 1000 times with the highest $R_{HRS/LRS}$ (5.5 vs. 2.5 order). Appropriate polarity SET bias applied on the RRAM and let the oxygen movement mainly in the insert rGO film, this operation shows the most stable HRS and higher $R_{HRS/LRS}$ (5 order) performance. Presumably, the oxygen rGO as the oxygen reservoir layer, enhanced the oxygen ion easy move in and out in the rGO film, and the rGO film also prevent the oxygen ion interactive with Al metal to degrade the $R_{HRS/LRS}$.

Acknowledgements

This work was supported by the National Science Council, ROC, under contract No. NSC 102-2221-E-035-081. We are also thankful to Dr. Cheng-Yu Hsieh of Energer Inc. Company supporting the rGO film deposition process.

References

- [1] K. M. Kim et al., *APL*, 91, 012907 (2007).
- [2] D. S. Jeong et al., *Nanotechnology*, 20, 375201 (2009).
- [3] H. Y. Lee et al., *IEDM*, 2008, p.297-300.
- [4] C. Chen et al., *JAP*, 111, 013702 (2012).
- [5] K. Kinoshita et al., *Solid State Electron.* 58, 48 (2011).
- [6] C. L. Lin et al., *SSDM*, Kyoto, 2012, pp.640-641.
- [7] J. Liu et al., *Adv. Mater.*, 25, 233-238 (2013).
- [8] H. Tian et al., *Nano Letters*, 13, 651-657 (2013).
- [9] M. H. Tang et al., *Microelectron. Eng.*, 93, 35-38 (2012).
- [10] B. Magyari-Kobe et al., *Nanotechnology*, 22, 254029 (2012).
- [11] M. Yi et al., *JAP*, 110, 063709 (2011).

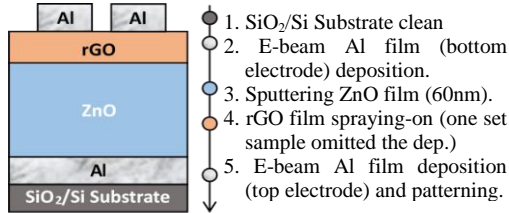


Fig. 1 The process and device structure of Al/rGO/ZnO/Al RRAM.

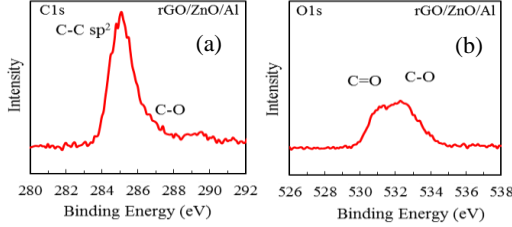


Fig. 2 The XPS analysis of the rGO film on ZnO/Al/SiO₂/Si substrate.

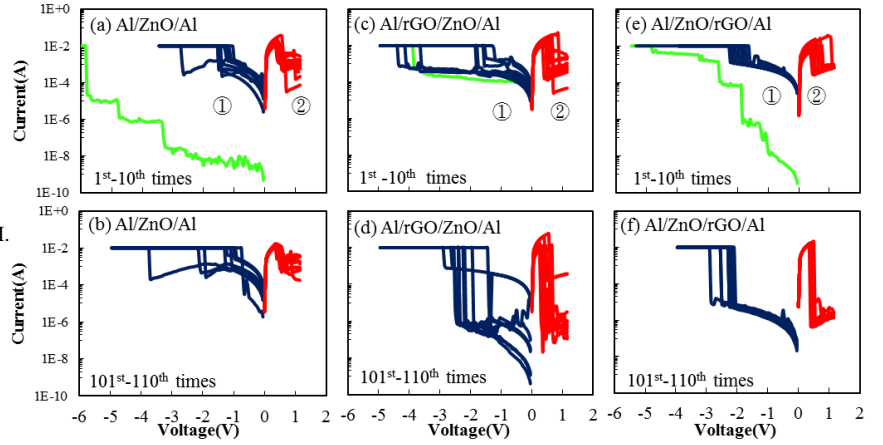


Fig. 3 The I-V characteristics of (a) 1st to 10th times and (b) 101st to 110th times of Al/ZnO/Al RRAM; (c) 1st to 10th times and (d) 101st to 110th times of Al/rGO/ZnO/Al RRAM; (e) 1st to 10th times and (f) 101st to 110th times of Al/ZnO/rGO/Al RRAM.

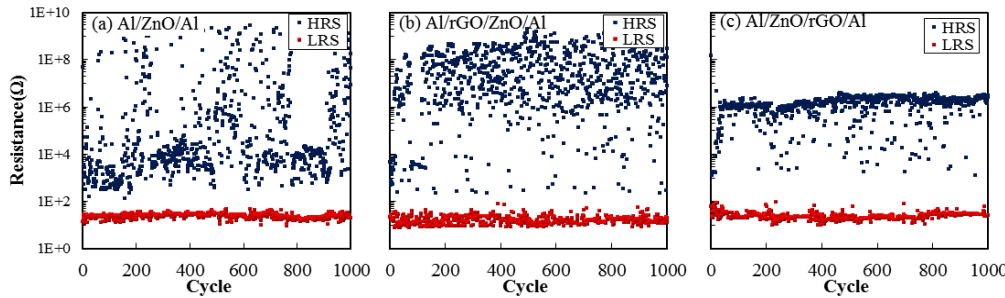


Fig. 4 The endurance of (a) Al/ZnO/Al, (b) Al/rGO/ZnO/Al and (c) Al/ZnO/rGO/Al RRAMs.

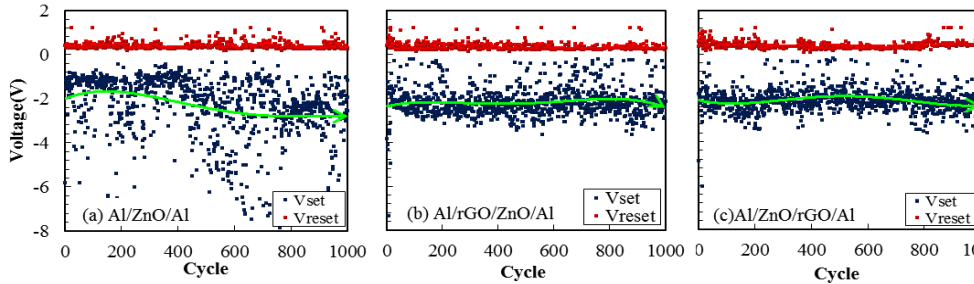


Fig. 6 The distributions of the SET and RESET voltages during the endurance testing of (a) Al/ZnO/Al, (b) Al/rGO/ZnO/Al, and (c) Al/ZnO/rGO/Al RRAMs under bipolar operation.

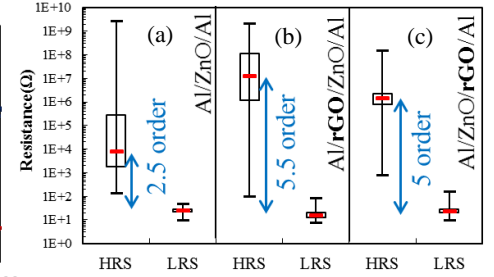


Fig. 5 The box-plot of HRS and LRS resistances of Al/ZnO/Al, Al/rGO/ZnO/Al and Al/ZnO/rGO/Al.

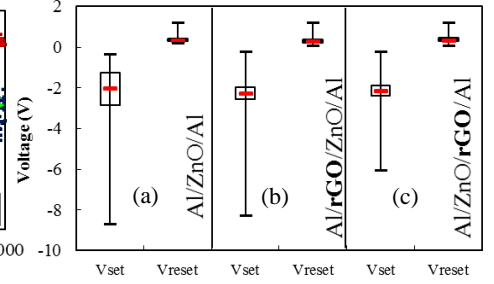


Fig. 7 The box-plot of SET/RESET voltages of Al/ZnO/Al, Al/rGO/ZnO/Al and Al/ZnO/rGO/Al RRAMs.

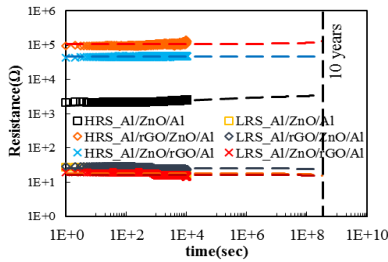


Fig. 8 The retention of Al/ZnO/Al, Al/rGO/ZnO/Al and Al/ZnO/rGO/Al RRAMs.

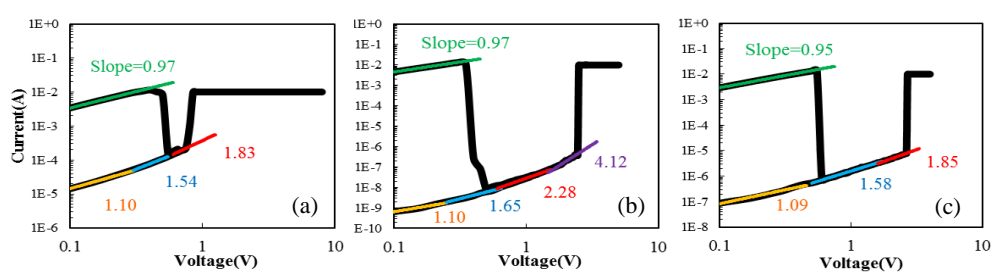


Fig. 9 Current transport behavior of (a) Al/ZnO/Al, (b) Al/rGO/ZnO/Al and (c) Al/ZnO/rGO/Al RRAMs.

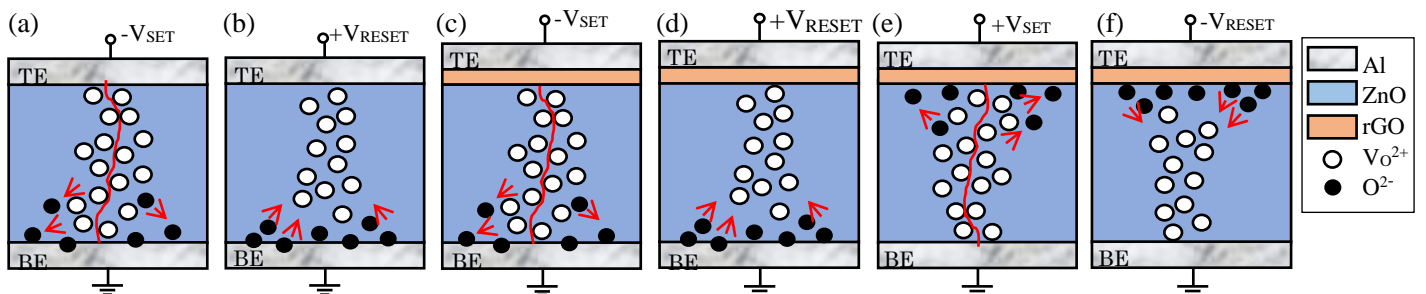


Fig. 10 Schematic bipolar switching mechanism (or conductive filament formation and rupture) of the generation and recombination of oxygen ions (O^{2-}) and oxygen vacancies ($V_{O^{2+}}$) for (a) the Al/ZnO/Al RRAM at SET (negative) and (b) RESET (positive) process, (c) the Al/rGO/ZnO/Al RRAM at SET (negative) and (d) RESET (positive) process and (e) the Al/ZnO/rGO/Al RRAMs at SET (positive) and RESET (negative) process (equivalent to negative SET bias applied on the bottom electrode).